



# DNA binding and dispersion activities of titanium dioxide nanoparticles with UV/vis spectrophotometry, fluorescence spectroscopy and physicochemical analysis at physiological temperature



Suhani Patel <sup>a</sup>, Palak Patel <sup>a</sup>, Sachin B. Undre <sup>b</sup>, Shivani R. Pandya <sup>c</sup>, Man Singh <sup>b,c</sup>, Sonal Bakshi <sup>a,\*</sup>

<sup>a</sup> Institute of Science, Nirma University, Ahmedabad 382481, Gujarat, India

<sup>b</sup> School of Chemical Sciences, Central University of Gujarat, Gandhinagar 382030, India

<sup>c</sup> Centre for Nano Science, Central University of Gujarat, Gandhinagar 382030, India

## ARTICLE INFO

### Article history:

Received 26 June 2015

Received in revised form 22 September 2015

Accepted 1 November 2015

Available online xxxx

### Keywords:

TiO<sub>2</sub> nanoparticles

Dispersion activities

DNA binding

Intermolecular interaction

*In vitro* assessment of genotoxicity

Bioavailability

## ABSTRACT

Overexposure of TiO<sub>2</sub> NPs has raised concerns over safety. This study focuses on stability and DNA binding activity of TiO<sub>2</sub> NPs in water and cell culture growth media RPMI-1640 at physiological temperature. Borosil Mansingh Survisometer was used to assess dispersion and physicochemical properties. Values of density, viscosity, surface tension, particle size, friccohesity and activation energy were calculated for a range of TiO<sub>2</sub> NP concentrations (25 μM/L to 125 μM/L). The results demonstrate higher limiting density and viscosity in culture media than water, suggesting a stronger association of TiO<sub>2</sub> NPs in growth media. Interaction of TiO<sub>2</sub> NPs with human genomic DNA was analyzed by UV–visible spectroscopy and fluorescence spectroscopy. UV–visible spectroscopy showed hyperchromic effect due to strong stacking interactions between human genomic DNA and TiO<sub>2</sub> NPs. Fluorescence spectral characteristics revealed that with increasing concentrations of TiO<sub>2</sub> NPs bound to DNA, there was a marked decrease in fluorescence spectra which indicates interaction of TiO<sub>2</sub> NP with human genomic DNA. Understanding structural and physicochemical properties of TiO<sub>2</sub> NPs and their interaction with human genomic DNA will be important for *in vitro* genotoxicity studies as stability of nano form in media is a major concern.

© 2015 Elsevier B.V. All rights reserved.

## 1. Introduction

Advancement of nanotechnology has led to production of nano materials with unique properties. The smaller size and larger surface area of NPs increase their biological reactivity. Hence there is increasing concern regarding potential adverse health effects of NPs on human body and environment at large [1,2,3,4]. TiO<sub>2</sub>, one of the most frequently used engineered metal oxide nanoparticle has a fundamental role as a white pigment. Due to its property of brightness, it is most favorable for use as an additive in paints, food coloring, cosmetics, sunscreens, toothpastes, polymers, medicines, ceramics & pharmaceutical industry [1,5,6,7]. Around 3000 t of TiO<sub>2</sub> NPs are produced globally every year and used in various fields due to high stability, photo catalytic properties and anti-corrosiveness [8,9]. TiO<sub>2</sub> occurs in 3 crystalline structures: Rutile, Anatase and Brookite. Rutile and Anatase are commercially available forms of TiO<sub>2</sub> NPs. Anatase is more chemically reactive whereas Rutile is considered to be stable [10,11]. Nanoparticles possess unusual physicochemical properties due to a variety of parameters such as

small size (surface area), surface structure (surface reactivity, surface groups), chemical composition (purity, crystallinity, electronic properties), shape, solubility, and agglomeration. Nanoparticles have the ability to bind and interact with biological matter changing the surface characteristics depending on the environment they are present, resulting in an increased concern over its potential effect on human body. Thus the characterization of nanoparticles in contact with the biological systems becomes complex leading to difficulty in classifying them as hazardous [12]. In 2006, the International Agency for Research on Cancer (IARC) reported sufficient evidence of carcinogenicity of TiO<sub>2</sub> in experimental animals and inadequate evidence of carcinogenicity in humans. Thus they declared it as group 2B carcinogen, “possibly carcinogenic to humans” [IARC 2010] [13,14]. Regulatory agencies seek laboratory data on toxicity of nanoparticles, in order to determine permissible limits in commercially available products. *In vitro* genotoxicity assessment requires addition of nanoparticles in growth media of proliferating cell cultures. Surface charge and other physicochemical properties of nanoparticles cause agglomerates, which can lead to non-nano size and thus change in characteristics. This can hamper the interpretation of biological effect of nanoparticles on cultured cells, like genotoxicity assessment. Attempts are going on to characterize the nanoparticles in culture media for extent of agglomeration, dispersion, and related properties, which can directly affect bioavailability

\* Corresponding author.

E-mail addresses: [suhanipalkhiwala@gmail.com](mailto:suhanipalkhiwala@gmail.com) (S. Patel), [palak608@gmail.com](mailto:palak608@gmail.com) (P. Patel), [sachincug@gmail.com](mailto:sachincug@gmail.com) (S.B. Undre), [shivpan02@gmail.com](mailto:shivpan02@gmail.com) (S.R. Pandya), [mansingh50@hotmail.com](mailto:mansingh50@hotmail.com) (M. Singh), [sonal.bakshi@nirmauni.ac.in](mailto:sonal.bakshi@nirmauni.ac.in) (S. Bakshi).

of nano form. The genotoxic effect of a compound can be exerted mainly by DNA interaction. Hence, we aim to study nanoparticles in culture media, for understanding *in vitro* genotoxicity. Reports suggest composition to be responsible for toxicity of conventional materials, where as physicochemical properties such as size, surface area, surface chemistry, surface roughness, medium of dispersion and ability to agglomerate are considered to be responsible for toxicity of nano materials [15]. Hence we aim to characterize nanoparticle dispersions and physicochemical parameters such as density, viscosity, surface tension, and activation energy in culture media. Since the physicochemical properties infer the level of solubility, reactivity, binding and dispersion of nanoparticles in medium, the critical evaluation of intermolecular interaction can be useful. Molecular distribution of nanoparticles is one of the contributory factors for agglomeration; with the culture medium or within NPs. This can be calculated with Einstein's equation considering  $r$  in nm [16]. The extent of dispersion in cell culture medium can be correlated with the extent of DNA binding, making it genotoxic. We aim to assess *in vitro* genotoxicity of TiO<sub>2</sub> NPs and hence decided to study the particokinetics and physicochemical properties in culture media. The present paper reports physicochemical properties of TiO<sub>2</sub> NPs dispersed in culture media RPMI-1640 and water, using Survimeter. We have also studied the interaction of DNA with TiO<sub>2</sub> NPs using UV-visible spectra and Fluorescence measurements.

## 2. Materials and methods

### 2.1. Materials

TiO<sub>2</sub> NPs manufactured by Sigma Aldrich (Cat. no. 634662) with a primary diameter of less than 100 nm were used. Tris-base, EDTA, Ethidium bromide, and RPMI-1640 media were purchased from Hi-Media. The human genomic DNA was isolated from normal WBCs of peripheral blood using the protocol of Qiagen's kit (Cat. no. 51104).

### 2.2. Methods

#### 2.2.1. Assessment of physicochemical properties by Borosil Mansingh Survimeter

The physicochemical properties such as density, viscosity, surface tension, activation energy, and friccohesity elucidate dispersion activities of TiO<sub>2</sub> in water and culture media. TiO<sub>2</sub> NPs suspensions were prepared at 25 μM, 50 μM, 75 μM, 100 μM and 125 μM concentrations in water as well as media. Densities were determined with Anton Paar Density and Sound velocity Meter (DSA 5000 M). Three mL suspension was filled in DSA Quartz U tube. Pendent drop numbers (PDN) and viscous flow times (VFT) were measured with Borosil Mansingh Survimeter (BMS) for assessment of surface tension and viscosity measurements respectively. To maintain physiological temperature of 37 °C, an auto temperature control LAUDA ALPHA RA 8 thermostat was used.

#### 2.2.2. Assessment of DNA binding activity by UV-visible measurements

UV absorption spectra of human genomic DNA suspension was studied at 256 nm, following addition of various concentrations of TiO<sub>2</sub> NPs. The spectrum was measured with Agilent Carry-60 UV visible spectrophotometer equipped with jacketed cell holders. Spectral changes of 13.71 μg DNA were monitored after adding various concentrations of TiO<sub>2</sub> NPs (0–200 μM) by recording the UV-visible absorption (200–700 nm). All experiments were run in Tris-base buffer (0.1 M), pH 7.5, in a conventional quartz cell attached with a thermostat to maintain the temperature at 37 °C. The absorbance profiles, which depict the thermal denaturation of DNA, were obtained using Carry-60 UV visible spectrophotometer, under controlled denaturation with change in temperature. Sample cells contained 13.71 μg DNA and 0 to 200 μM TiO<sub>2</sub> NPs. The recording chart read temperature and absorbance differences between the reference cuvettes (which were the same as the sample

except the DNA and DNA with TiO<sub>2</sub> NPs at increasing concentrations were noted).

#### 2.2.3. Assessment of DNA binding activity by Fluorescence measurements

Fluorescence quenching helps in understanding the interaction of chemical with DNA. Ethidium bromide binds to DNA by inserting between the stacked bases and fluoresces due to the hydrophobic environment between base pairs. In this assay, 100 μg of DNA was added to 2-μM aqueous Ethidium bromide with maximum quantum yield at 471 nm, hence this wavelength was selected as the excitation wavelength for samples at 37 °C in the range 500–720 nm. Different volumes of TiO<sub>2</sub> NPs (1–140 μL) were added to the DNA suspension containing Ethidium bromide and measurements were done using a 1 cm path length fluorescence cuvette. At the highest denaturation concentration and an excitation wavelength of 471 nm, the fluorescence intensities of TiO<sub>2</sub> NPs were checked and the emission intensities were recorded.

## 3. Results and discussion

### 3.1. Physicochemical study

Intermolecular forces (IMF) like Dipole–Dipole, Ion–Dipole, Dipole-induced Dipole and London dispersion forces catalyze interaction or dispersion between two molecules. Physicochemical properties of dispersed molecules and the media in which they are dispersed determine the IMF monitored reactions. We study the density, viscosity, surface tension, friccohesity, activation energy and molecular radii of TiO<sub>2</sub> NPs dispersed in water and media at 37 °C.

#### 3.1.1. Density

Density is defined, as mass per unit volume, and intermolecular forces are the forces of attraction that hold the molecules together. Density, which depicts internal pressure of the TiO<sub>2</sub> NPs in water and media, is regressed with mM/L using following Eq. (1).

$$\rho = \rho^0 + S_p m + S'_p m^2 \quad (1)$$

$\rho^0$  at  $m \rightarrow 0$  is limiting density and  $S_p$  is the 1st slope. A stronger intermolecular force between the components of RPMI-1640 media and TiO<sub>2</sub> NPs causes higher density of media as compared to the TiO<sub>2</sub> NPs in water. There is an interaction-taking place between metallic Titanium with the components of media resulting in shorter intermolecular distances. Therefore the molecules in the media are densely packed and held together by ionic force of attraction. The stronger intermolecular forces in media components pull TiO<sub>2</sub> NPs towards it, resulting in more molecules per unit volume. The density (1.0067 kg m<sup>-3</sup>) of RPMI-1640 media is 1.36% higher as compared to water (0.9930 kg m<sup>-3</sup>) due to composition of the media. An increase in the density of water and media is observed with increase in TiO<sub>2</sub> NP concentrations (Table 2, Fig. 1). TiO<sub>2</sub>-media (1.0031 kg m<sup>-3</sup>) has a higher limiting density than TiO<sub>2</sub>-water (0.9937 kg m<sup>-3</sup>), due to the presence of TiO<sub>2</sub> NPs in media, explaining a 0.84% stronger intermolecular force interaction between TiO<sub>2</sub> NPs and media than water. The 0.00002 kg<sup>2</sup> m<sup>-3</sup> mol<sup>-1</sup> and 0.000008 kg<sup>2</sup> m<sup>-3</sup> mol<sup>-1</sup> slope ( $S'_p$ ) values of TiO<sub>2</sub>-media and TiO<sub>2</sub>-water respectively, show TiO<sub>2</sub>-media > TiO<sub>2</sub>-water indicating composition effects of media is higher as compared to water (Table 3a). Thus for dispersion studies it can be inferred that

**Table 1**

Density ( $\rho \pm 10^{-3}$  kg m<sup>-3</sup>), viscosity ( $\eta \pm 10^{-5}$  mPa·s) and surface tension ( $\gamma \pm 10^{-2}$  mN m<sup>-1</sup>) of pure water and RPMI-1640 media at 310.15 K.

Pure solvents	$\rho$	$\eta$	$\gamma$
Water	0.9930	0.6960	70.00
RPMI-1640 media	1.0067	0.7312	63.40

**Table 2**

Micro molar/L ( $\mu\text{M}$ ), density ( $\rho \pm 10^{-3} \text{ kg m}^{-3}$ ), viscosity ( $\eta \pm 10^{-5} \text{ mPa}\cdot\text{s}$ ), surface tension ( $\gamma \pm 10^{-2} \text{ mN m}^{-1}$ ), friccohesity ( $\sigma, \text{ s.m.}^{-1}$ ), activation energy ( $\Delta\mu_2^\ddagger \pm 10^{-2} \text{ kJ mol}^{-1}$ ), molecular radii ( $r, \text{ nm}$ ) at 310.15 K.

$\mu\text{M}$	$\rho$	$\eta$	$\gamma$	$\sigma$	$\Delta\mu_2^\ddagger$	$r$
<i>TiO<sub>2</sub> + water</i>						
25	0.9939	0.657909	70.59	0.0132975	-57.72	10.84
50	0.9940	0.673002	70.60	0.01360118	-57.68	8.60
75	0.9943	0.682157	70.62	0.01378204	-57.67	7.51
100	0.9945	0.684781	70.63	0.01383228	-57.66	6.83
125	0.9946	0.709890	70.64	0.01433804	-57.63	6.34
<i>TiO<sub>2</sub> + RPMI media</i>						
25	1.0034	0.75417132	63.62	0.015750	-57.67	10.80
50	1.0043	0.75565758	63.25	0.015872	-57.69	8.57
75	1.0046	0.75562293	63.27	0.015867	-57.72	7.49
100	1.0052	0.75711633	63.73	0.015783	-57.78	6.80
125	1.0054	0.75703535	63.74	0.015778	-57.83	6.31

increased density of media results in higher binding interactions of TiO<sub>2</sub> NPs in media as compared to water. See Table 1

Since water exhibits repelling nature towards TiO<sub>2</sub>, the NPP remain suspended and get settled down indicating lower density (Tables 2, 3a; Fig. 1). Where as in media, TiO<sub>2</sub> NPs get uniformly bound to its components, due to which the structure gets aggregated to develop stronger interactions.

### 3.1.2. Viscosity

Viscosity is a flow property governed by frictional forces (FF), defined as the resistance of a liquid to flow. In this study, it reflects the effect of IMF on flow, due to entanglement of TiO<sub>2</sub> with the components of water and RPMI-1640 media. Viscosity increases with increasing strength of IMF. It is observed that viscosity of TiO<sub>2</sub> in media is higher than in water (Fig. 2). The viscosities were calculated for 25  $\mu\text{M}$  to 125  $\mu\text{M}$  concentrations of TiO<sub>2</sub> in water and media separately, from their viscous flow times ( $t$ ) with following Eq. (2).

$$\eta = \left(\frac{t}{t_0}\right) \left(\frac{\rho}{\rho_0}\right) \eta_0 \quad (2)$$

$\eta_0$  is viscosity for water and RPMI-1640 is dispersing medium, the  $t_0$  and  $t$  are flow times of solvent and mixtures respectively. The  $\eta$  data were regressed with mM/L with following Eq. (3).

$$\eta = \eta^0 + S_\eta m \quad (3)$$

$\eta^0$  at  $m \rightarrow 0$  is limiting viscosity;  $S_\eta$  is the 1st degree slope for effect of composition on interaction. The viscosities increase with increase in

**Table 3a**

Limiting density ( $\rho^0, \text{ kg m}^{-3}$ ), 1st slope ( $S_\rho, \text{ kg}^2 \text{ m}^{-3} \text{ mol}^{-1}$ ), Limiting viscosity ( $\eta^0, \text{ mPa}\cdot\text{s}$ ), 1st slope ( $S_\eta, \text{ mPa}\cdot\text{s kg m}^{-1}$ ), Limiting surface tension ( $\gamma^0, \text{ mN m}^{-1}$ ), 1st slope ( $S_\gamma, \text{ mN kg mol}^{-1} \text{ m}^{-1}$ ).

System	$\rho$		$\eta$		$\gamma$	
	$\rho^0$	$S_\rho$	$\eta^0$	$S_\eta$	$\gamma^0$	$S_\gamma$
TiO <sub>2</sub> + water	0.9937	0.000008	0.6468	0.0005	70.577	0.0005
TiO <sub>2</sub> + RPMI	1.0031	0.000002	0.7538	0.00003	63.306	0.0029

concentration of TiO<sub>2</sub> NPs in media and water (Table 2, Fig. 2). Their limiting viscosities were found to be 0.7538 mPa·s and 0.6468 mPa·s with TiO<sub>2</sub>-media and TiO<sub>2</sub>-water respectively (Table 3a). We observed a positive slope ( $S_\eta$ ) for TiO<sub>2</sub> NPs in media (0.0005 mPa·s kg m<sup>-1</sup>) and TiO<sub>2</sub> NPs in water (0.00003 mPa·s kg m<sup>-1</sup>) (Table 3a) indicating structure breaking and making effect (Table 3a). This suggests that water shows higher structure breaking effect while culture media shows the structure making effects with TiO<sub>2</sub> NPs. RPMI-1640 media has various components, which are adjacent to each other increasing the point of contact. This causes more interaction of the components with TiO<sub>2</sub> NPs, which is reflected in higher viscosity of media.

### Composition of RPMI-1640 media

Fetal bovine serum, which is harvested from Bovine fetuses taken from pregnant cows during slaughter, is one of the major components in RPMI-1640 media. It is the portion of plasma remaining after coagulation of blood. Plasma protein fibrinogen is converted into fibrin during coagulation. FBS is preferred since it has low level of antibodies and more growth factors, allowing versatility in many different cell culture applications. Globular protein Bovine Serum Albumin constitutes a major component in FBS. Thus, more the numbers of these constituents in media, higher will be the concentration. This would lead to more interaction due to increased availability. Hence an effect of composition is reflected in an increase in density and viscosity of media containing TiO<sub>2</sub> NPs.

### 3.1.3. Surface tension

Surface tension is a cohesive property in which molecules or particles sustain cohesivity with a uniform molecular arrangement in the medium. Cohesive forces (CF), existing between molecules of the same kind or similar substance are also the function of IMF. These forces cause a tendency in liquids to resist separation. Surface tension data for 25  $\mu\text{M}$  to 125  $\mu\text{M}$  of TiO<sub>2</sub> NPs with 25  $\mu\text{M}$  intervals in water and culture media are calculated with following Eq. (4).

$$\gamma = \left(\frac{\eta_0}{\eta}\right) \left(\frac{\rho_0}{\rho}\right) \gamma_0 \quad (4)$$

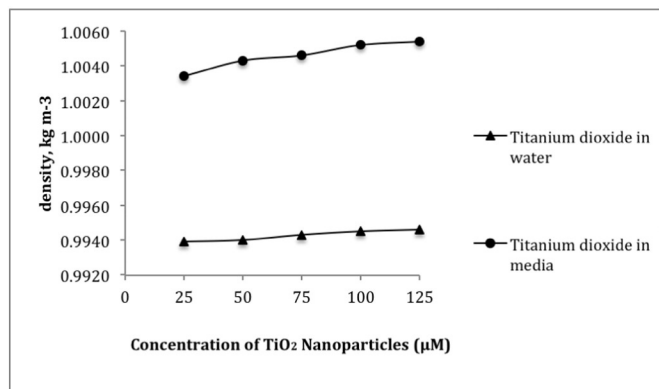


Fig. 1. Density of TiO<sub>2</sub> in water and media.

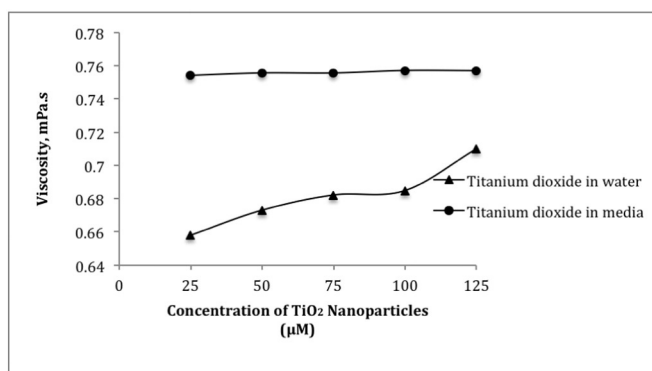


Fig. 2. Viscosity of TiO<sub>2</sub> in water and media.

$\gamma_0$  is surface tension of medium.  $n_0$  and  $n$  are pendant drop numbers of medium and solutions respectively. The  $\gamma$  data are regressed for limiting values  $\gamma^0$  at  $m \rightarrow 0$  with following Eq. (5).

$$\gamma = \gamma^0 + S_\gamma m \quad (5)$$

$\gamma^0$  is limiting surface tension, and  $S_\gamma$  is the 1st degree slope  $\text{TiO}_2$  NP dispersions. A pattern of change in surface tension was observed (Fig. 3). It can be inferred that  $\text{TiO}_2$  NPs favor interactions responsible for the dispersion. Thus, more numbers of  $\text{TiO}_2$  NP, at higher concentration, increase the interaction due to more availability for dispersion. Limiting surface tension for  $\text{TiO}_2$  NPs in water and  $\text{TiO}_2$  NPs in media is  $70.577 \gamma^0$ ,  $\text{mN m}^{-1}$  and  $63.306 \gamma^0$ ,  $\text{mN m}^{-1}$  respectively. It is observed that water has surface tension of  $70 \text{ mN/M}$ , because of strong attractive forces on its surface forming a spherical shape resulting in a smaller surface area for the given volume. Water molecules are bonded to each other by a hydrogen bond existing between H atoms on a molecule and O atoms of another molecule.

While in media, mismatch in the molecules is not so much since there is a weak attractive force between molecules, there is lesser intermolecular force attraction in media and therefore media has surface tension of  $63.71 \text{ mN/M}$  at  $37^\circ\text{C}$ . The added  $\text{TiO}_2$  NPs are attached to media components and water. NPs have a polar head to which the water component of media gets attracted and a hydrophobic nonpolar part, which is attached to media components. The presence of these substances weakens the strength of the layer and they interfere with H bond existing between water molecules of media. In media, a portion of the nanoparticle-organic components present, tend to get aggregated at the surface of water, and their non-polar tail sticks out away from water. At the surface, these molecules interfere with Dipole–Dipole interactions amongst water molecules, thereby reducing surface tension.

### 3.1.4. Friccohesity

Friccohesity is a dual force theory, considered to be the product of frictional force and cohesive force within similar or dissimilar molecules. A cohesive force exists between the water molecules and nanoparticles. The force gets weakened when frictional force begins to develop at the same level. Therefore the forces are interrelated with each other. Friccohesity was calculated using Mansingh Eq. (6) [27].

$$\sigma = \sigma_0 \left[ \left( \frac{t}{t_0} \pm \frac{B}{t} \right) \left( \frac{\eta}{\eta_0} \pm 0.0012(1 - \rho) \right) \right] \quad (6)$$

[17].

Here,  $\sigma$  is a friccohesity,  $\sigma^0$  is a reference friccohesity,  $t$  and  $t_0$  are the solution and sample viscous flow times respectively.  $n_0$

and  $n$  are the pendant drop number of reference and solutions respectively.

$$\sigma = \sigma_0 \left[ \left( \frac{t}{t_0} \right) \left( \frac{\eta}{\eta_0} \right) \right] \quad (7)$$

Reference friccohesity was calculated by  $\sigma^0 = \eta_0/\gamma_0$ , where  $\eta_0$  and  $\gamma_0$  are the viscosity and surface tension of references (water and media) respectively (Table 3b). A combination of frictional force and cohesive force reflects the state of interaction of the molecules.

There is an increase in friccohesity values, with increasing concentrations of  $\text{TiO}_2$  NPs in water and media (Fig. 4). The limiting friccohesity was found to be higher in the case of  $\text{TiO}_2$  NPs-media ( $0.0158 \text{ s.m.}^{-1}$ ) as compared to  $\text{TiO}_2$  NPs-water ( $0.0131 \text{ s.m.}^{-1}$ ) (Table 3b, Fig. 4). Friccohesity of  $\text{TiO}_2$  NPs-media is higher since, there is stronger interconversion of cohesive force to frictional force due to bulkiness of the media. The value rises with increasing concentration of interconversion of cohesive force to frictional force. This leads to stronger frictional force at the cost of cohesive force with stronger NP-media interaction. The decreased values depict weaker  $\text{TiO}_2$  NP-water interaction due to weakening of the frictional force between nanoparticle and water molecules. Weakening of the cohesive force between water molecules with lower product of intermolecular forces also contributes to the decrease in friccohesity. The slope values also support this structural circumstance (Table 3b).

### 3.1.5. Activation Energy

Activation energy is the minimum amount of energy needed, in order to carry out a chemical reaction. At lower activation energy, greater proportion of the collisions between solute and the solvent will result in reaction. A free reaction is favorable if the free energy difference between products and reactants is negative. The partial molar volume  $V_2$  was calculated with following Eq. (8).

$$V_2 = \left[ \frac{1000(\rho^0 - \rho)}{m\rho^0\rho} \right] + \frac{M}{\rho} \quad (8)$$

$M$  molar mass,  $\rho_0$  density of water and  $\rho$  is density of solution. The  $V_1$  for water and media at  $37^\circ\text{C}$  is calculated with Eq. (9).

$$V_1 = \frac{M}{\rho} \quad (9)$$

$V_1$  and  $V_2$  are used for activation energy [24] obtained from Eq. (10).

$$\Delta\mu_1^* = RT \ln \left( \frac{\eta_0 V_1}{hN} \right) \quad (10)$$

$\Delta\mu_1^*$  is activation energy for water and media,  $R$  is gas constant,  $h$  is Planck constant and  $N$  is Avogadro number ( $6.023 \times 10^{23}$ ). Activation energy ( $\Delta\mu_2^*$  J/mol) was calculated with Eq. (11) [18].

$$\Delta\mu_2^* = \Delta\mu_1^* - \left[ \left( \frac{Rt}{V_2} \right) ((1000\eta) - (V_1 - V_2)) \right] \quad (11)$$

**Table 3b**

Limiting friccohesity ( $\sigma^0$ ,  $\text{s.m.}^{-1}$ ), 1st slope ( $S_\sigma$ ,  $\text{s.m.}^{-1} \text{ kg}^2 \text{ mol}^2$ ), Limiting activation energy ( $\Delta\mu_2^{*0}$ ,  $\text{kJ mol}^{-1}$ ), 1st slope ( $S\Delta_{i2}^*$ ,  $\text{kJ L/mM}^2$ ), Limiting molecular radii ( $r^0$ , nm), 1st slope ( $S_r$ , nm).

System	$\sigma^0$		$\Delta\mu_2^{*0}$		$r^0$	
	$\sigma^0$	$S_\sigma$	$\Delta\mu_2^{*0}$	$S\Delta_{i2}^*$	$r^0$	$S_r$
$\text{TiO}_2 + \text{water}$	0.0131	0.000009	-57.732	0.0008	11.255	-0.0431 ×
$\text{TiO}_2 + \text{RPMI}$	0.0158	0.0000001	-57.615	-0.0016	11.219	-0.043 ×

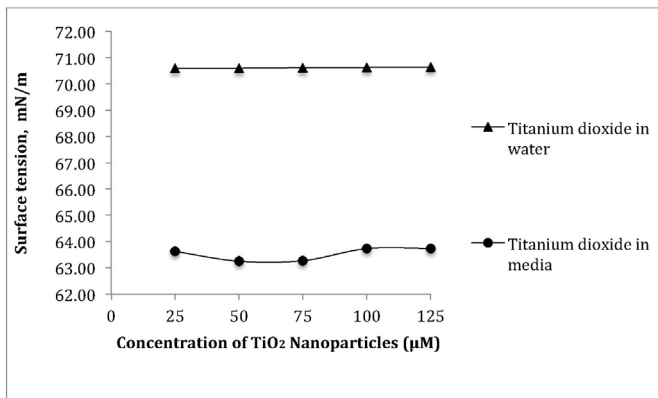


**Fig. 3.** Surface tension of  $\text{TiO}_2$  in water and media.

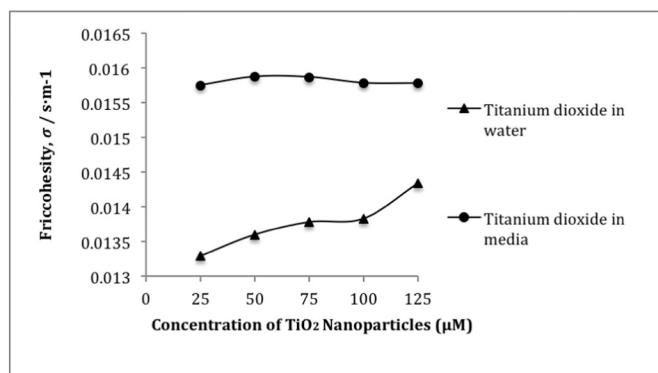


Fig. 4. Friccohesity of TiO<sub>2</sub> in water and media.

The limiting values are given in the Table 3b.

Activation energy of nanoparticles in media is lesser than that in water, which results in its faster and more spontaneous dispersion in media compared to water (Fig. 5). A substantial amount of inorganic soluble salts present in media contribute to its higher ionic strength, creating a favorable environment for molecular interactions. In addition to this, since there are more molecules present in the aqueous media, increased chances of collisions significantly increase the molecular interactions. Stabilizing interaction between nanoparticles and media components need higher energy utilization leading to a decrease in activation energy. Stronger media NP interaction is also indicated by an increase in density and viscosity as stated above.

### 3.1.6. Molecular radii

Molecular radii play an important role in the dispersion activities of NPs in water and media. The molecular radii  $r$  in nm is calculated with Eq. (12).

$$r = \sqrt[3]{\frac{3\phi}{4\pi N_A c}} \quad (12)$$

$\phi$  is volume fraction of water and media entangled with NPs.  $N_A$  is Avogadro number,  $c$  is concentration,  $\pi$  is constant and the  $r$  data are given in Tables 2, 3b and Fig. 6. Since there is no significant difference in the molecular radii observed in the case of TiO<sub>2</sub> NPs dispersed in water and media, we infer TiO<sub>2</sub> NPs disperse in water and media with the same proportion (Fig. 6). Their limiting radii ( $r$ ) were found to be 11.219 nm and 11.255 nm for TiO<sub>2</sub> NP-media and TiO<sub>2</sub> NP-water respectively indicating the cage formation of TiO<sub>2</sub> NP with media and water (Table 3b).

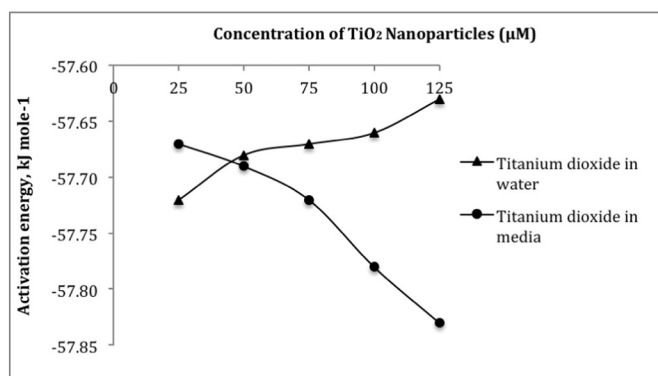


Fig. 5. Activation energy of TiO<sub>2</sub> in water and media.

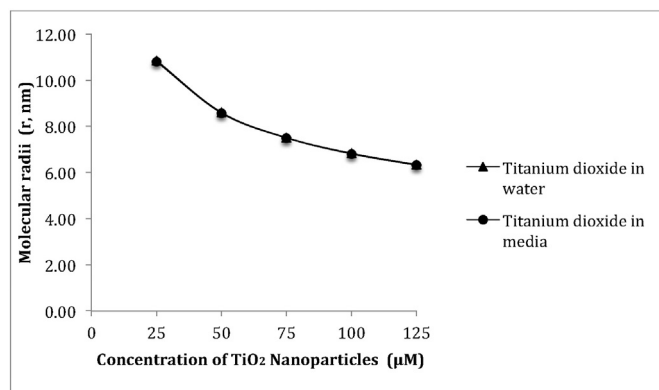


Fig. 6. Molecular radii of TiO<sub>2</sub> in water and media.

### Media

HiKaryoXL™ RPMI Medium is a medium developed for short term *in vitro* culture of peripheral blood lymphocytes. It is mainly used for cytogenetic studies like Genotoxicity i.e. study of metaphase chromosomal aberrations in terms of structural and numerical abnormalities. Lymphocytes from normal peripheral blood need mitogenic stimulation hence Phytohemagglutinin (PHA-M) is added in the HiKaryoXL™ RPMI-1640 Medium (AL165A). This is a basal medium supplemented with L-Glutamine, Fetal bovine serum, PHA-M, Penicillin, Streptomycin, and Sodium bicarbonate. It also consists of inorganic salts, amino acids, vitamins, antibiotics and D-Glucose.

### 3.2. UV vis studies

The interaction of TiO<sub>2</sub> NPs with human genomic DNA has been studied with UV-visible spectroscopy in order to investigate the possible binding of nanoparticle to DNA. Interaction of DNA with TiO<sub>2</sub> NPs is studied by recording the absorption spectra for a constant DNA concentration in various TiO<sub>2</sub> NPs mixing ratios at 37 °C, the results of which are shown in Fig. 7. Absorption Spectroscopy helps to determine the binding characteristics of metal complexes with DNA. The spectral changes observed in the form of 'hyperchromism' and 'hypochromism' during the process, reflect the change in conformation of DNA and structure of DNA [19]. Metal complex can bind to the DNA *via* covalent and or/non-covalent interactions [20]. DNA base pairs have strong optical absorption at approximately 260 nm. The absorption spectra of DNA in absence and presence of TiO<sub>2</sub> NPs is shown in Fig. 7a. With addition of increasing amounts of TiO<sub>2</sub> NPs to DNA, there is an increase in absorbance observed, up to 15.3%, without any shift in the maxima wavelength of 256 nm. Hyperchromism is reported to suggest breakage of the secondary structure of DNA, and therefore this hyper chromic effect suggests there exists a strong interaction between nanoparticles and the human genomic DNA [21]. The binding results of which are shown in the Fig. 7b. The metal complex can bind to DNA *via* covalent and or/non-covalent interactions. Covalent interactions include *via* alkylation or inter and intra strand crosslinking [22]. Non-covalent interactions include the following:

1. Intercalation between the base pairs
2. Binding to the major groove, minor groove or sugar phosphate backbone
3. Binding to the exterior of the helix through non-specific interactions, which are electrostatic [33,34].

Non covalent DNA interacting agents can change DNA conformation, change DNA torsional tension, interrupt protein-DNA interactions and potentially lead to DNA strand breaks, which is one of the end point of genotoxicity [22,23,25].

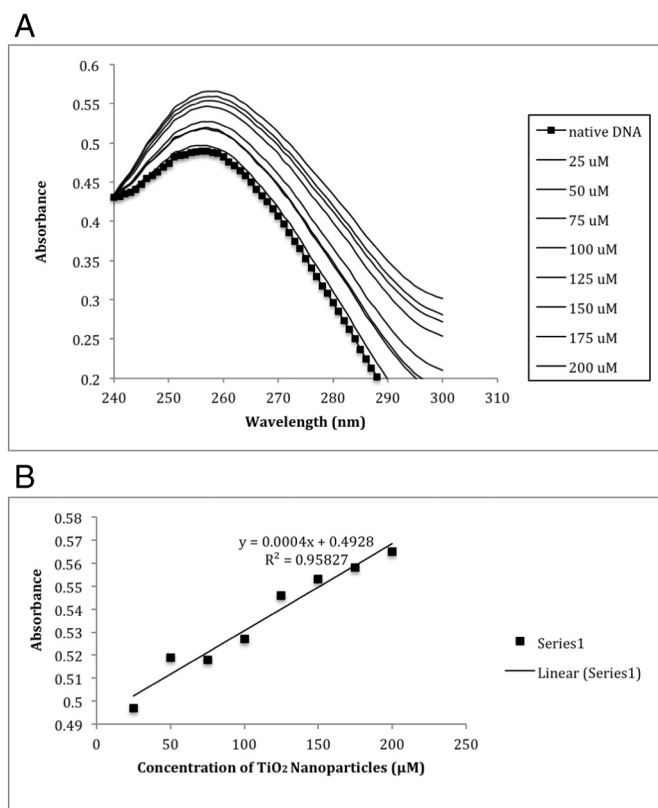


**Fig. 7.** a. Changes of UV spectra of human genomic DNA in the presence of different concentrations of TiO<sub>2</sub> nanoparticle in Tris-base buffer (0.1 M), pH 7.5 at 37 °C. b. alterations in maximum absorbance (at 256 nm) of human genomic DNA in the presence of different concentrations of TiO<sub>2</sub> nanoparticles.

We hypothesize various modes in which the nanoparticles bind to the DNA, resulting in an increase in absorbance.

- (1). The absorption intensity at 256 nm is increased due to exposure of purine and pyrimidine bases of DNA when TiO<sub>2</sub> NPs bind to DNA. This method of binding could have caused a slight change in the conformation of DNA [21].
- (2). In presence of electrostatic interaction created between TiO<sub>2</sub> NPs and DNA, there can be conformational and structural changes that take place in DNA. Stacking interactions, hydrogen bonds, and hydrophobic effect between complementary bases holds the two strands of DNA together. Addition of TiO<sub>2</sub> NP, results in base–base interaction being reduced in DNA, due to which many bases would be in free form and H bonding is not present between complementary bases. This leads to an increase in UV absorbance. As a result, absorbance for a single stranded DNA will be 40% higher than that of double stranded DNA at the same concentration [26]. We hypothesize an interaction mechanism between TiO<sub>2</sub> NPs and the phosphate backbone of DNA. Charged cation Ti can bind to phosphate group of DNA backbone via electrostatic as depicted in the graphical figure abstract. Each strand of the DNA backbone consists of de-oxy ribose sugar molecules (A, G, C, T) which are linked together by phosphate groups that possess C–O–P and P=O as binding site. The 3′C of a sugar molecule is connected through a phosphate group to 5′C of the next sugar by a phosphodiester bond. Since the phosphate backbone is negatively charged, it can attract positively charged TiO<sub>2</sub> NPs. Ti–O is considered to be the major component of TiO<sub>2</sub> NP and thus will react with P=O to form P–O–Ti–O, loosening C–O–P bond, as shown in the graphical figure abstract [27]. There is a possibility that the other O atom, which is a part of TiO<sub>2</sub> NP, be released as an oxygen ion (reactive oxygen species).

Reports suggest TiO<sub>2</sub> NPs release ROS, thus resulting in oxidative damage; cytotoxicity and DNA damage eventually leading to genotoxicity [28,29,30,31].

- (3). Hyperchromism can also be due to the external contact or partial uncoiling of the helix structure of DNA, exposing more bases of the DNA [25,32,33]
- (4). The other possibility of hyperchromism can be rationalized in terms of groove binding. Since an aromatic ring closely matching with the helical turn is a required to be a part of the metallic compound, this possibility seems unlikely [25].

It has been reported that hypochromism is due to the intercalative mode involving a strong stacking interaction between an aromatic chromophore of a drug and base pairs of DNA [25]. The above explanations indicate there might be an electrostatic interaction between the TiO<sub>2</sub> NP and human genomic DNA. And since hyperchromism is observed, we can conclude that TiO<sub>2</sub> NP binds to the DNA for certain, causing a conformational change.

### 3.3. Fluorescence measurements

Fluorescence quenching is studied by a fluorescence titration spectrum, which is an effective method to study the reactivity of chemical and biological systems, by allowing non-intrusive dimensions of substances in low concentration under physiological conditions. It also helps in providing information about binding mechanisms and the nature of binding [34,35]. The experiment is performed using Ethidium bromide (EB), a common DNA binding fluorophore with increasing concentrations of TiO<sub>2</sub> NPs, to determine the extent of binding of nanoparticles and human genomic DNA. EB strongly fluoresces in presence of DNA due to intercalation between the adjacent DNA base pairs. It has been previously reported that this enhanced fluorescence can be quenched by the addition of a second molecule. With the addition of a second molecule, there will be a competition between EB and the second molecule to bind to human genomic DNA. This leads to a decrease in fluorescence intensity. The extent of fluorescence quenching of EB bound to human genomic DNA can be used to determine the binding of second molecule with human genomic DNA. The emission spectra of EB bound to human genomic DNA in absence and presence of TiO<sub>2</sub> NPs has been reported. The fluorescence emission spectra of intercalated Ethidium with increasing concentrations of TiO<sub>2</sub> NPs at 37 °C are shown in Fig. 8a. The fluorescence intensity of EB–DNA decreases with increasing concentrations of Titanium dioxide nanoparticles at physiological temperature 37 °C (Fig. 8b). This decrease of EB fluorescence (up to 27.49% of the initial EB–DNA fluorescence intensity) indicates competition of TiO<sub>2</sub> NPs with EB in binding to DNA. It can be concluded that fluorescence intensity of DNA intercalated by Ethidium is quenched when Ethidium is removed from the duplexes by action of TiO<sub>2</sub> NPs. These results suggest that TiO<sub>2</sub> NPs intercalate the DNA strands. The fluorescence quenching efficiency can be described by the Stern–Volmer equation:

$$\frac{I_0}{I} = 1 + K_{sv} [\text{Titanium dioxide nanoparticle}]$$

where I<sub>0</sub> and I represent the fluorescence intensities in the absence and presence of TiO<sub>2</sub> NPs, respectively and K<sub>sv</sub> is a linear Stern–Volmer quenching constant. K<sub>sv</sub> value calculated from the plot is shown in the Fig. 8c of I<sub>0</sub>/I versus Titanium dioxide nanoparticle concentrations. The value of Stern–Volmer quenching constant (K<sub>sv</sub>) was found to be 1.6 mM<sup>−1</sup> (R = 0.98592). The quenching of fluorescence of EB bound to human genomic DNA by TiO<sub>2</sub> NPs is in good agreement with the linear Stern–Volmer equation, which provides evidence that there is partial replacement of EB bound to DNA by nanoparticle, resulting in decreased fluorescence intensity resulting in a decrease of fluorescence

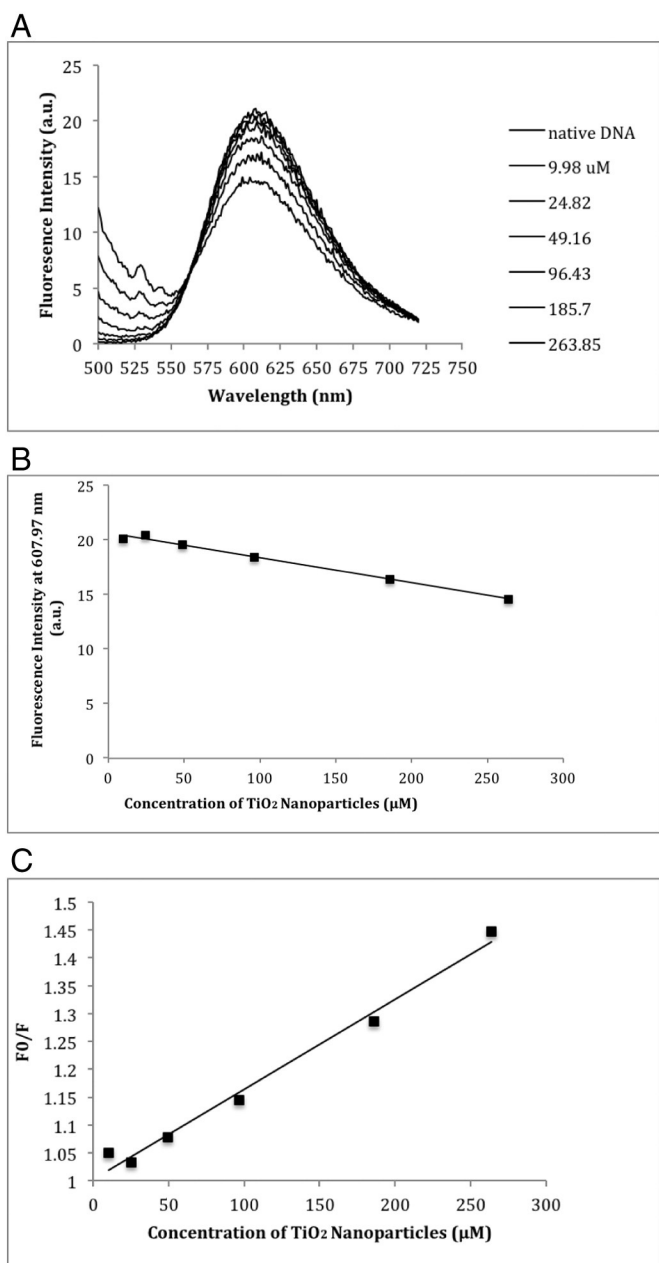


**Fig. 8.** a. Fluorescence emission spectra of intercalated Ethidium bromide incubated with human genomic DNA by increasing concentrations of TiO<sub>2</sub> nanoparticle at 37 °C. b. Alterations in the Ethidium bromide fluorescence at different concentrations of TiO<sub>2</sub> nanoparticles. c. Stern–Volmer plot of DNA-EB in the presence of different concentrations of TiO<sub>2</sub> nanoparticle.

intensity. The data suggests interaction of TiO<sub>2</sub> NPs to the DNA. [21,25,36].

#### 4. Conclusion

The results of density, viscosity and friccohesity measurement show that intermolecular interactions of TiO<sub>2</sub> NPs with media are higher as compared to water, indicating greater dispersion and molecular interaction. The mono dispersed status of TiO<sub>2</sub> NPs in culture media suggests better correlation with biological effect. Hyperchromic effect observed in UV–visible studies indicates an electrostatic interaction between TiO<sub>2</sub> NPs and DNA. Fluorescence spectroscopy exhibits an appreciable decrease in emission upon addition of TiO<sub>2</sub> NPs, as Ethidium bromide gets displaced from the DNA duplex, and TiO<sub>2</sub> NPs intercalates within

it. From the above results it can be concluded that binding of TiO<sub>2</sub> NPs to DNA results in structural changes in DNA. We have undertaken assessment of induced chromosomal damage in similar conditions. The biological effect of nanoparticles should be correlated with well-characterized physicochemical properties when addressing human toxicological responses. Our study reports dispersion activities and binding of nanoparticles with DNA, which will help in better understanding of *in vitro* genotoxicity since the genotoxic potential of a compound is largely due to its DNA binding capacity.

#### Acknowledgments

We would like to thank Dr. Mill Das for her kind help and Nirma University for the financial support.

#### References

- [1] G. Oberdörster, E. Oberdörster, J. Oberdorster, Nano-toxicology: an emerging discipline evolving from studies of ultrafine particles, *Environ. Health Perspect.* 113 (2005) 823–839.
- [2] S.T. Stern, S.E. McNeil, Nanotechnology safety concerns revisited, *Toxicol. Sci.* 101 (2007) 4–21.
- [3] L.K. Limbach, P. Wick, P. Manser, R.N. Grass, A. Bruinink, W.J. Stark, Exposure of engineered nanoparticles to human lung epithelial cells: influence of chemical composition and catalytic activity on oxidative stress, *Environ. Sci. Technol.* 41 (2007) 4158–4163.
- [4] C.W. Lam, J.T. James, R. McCluskey, R.L. Hunter, Pulmonary toxicity of single-wall carbon nanotubes in mice 7 and 90 days after intratracheal instillation, *Toxicol. Sci.* 77 (2004) 126–134.
- [5] J. Fisher, T.A. Egerton, Titanium compounds, inorganic, *Kirk-Othmer Encyclopedia of Chemical Technology*, John Wiley & Sons, New York, 2001 (on-line).
- [6] M.J. Khan, M.Y. Maskat, Interaction of titanium dioxide nanoparticle with human serum albumin: a spectroscopic approach, *Int. J. Pharm. Pharm. Sci.* 6 (2014) 3.
- [7] M.C. Lomer, C. Hutchinson, S. Volkert, S.M. Greenfield, A. Catterall, R.P. Thompson, J.J. Powell, Dietary sources of inorganic microparticles and their intake in healthy subjects and patients with Crohn's disease, *Br. J. Nutr.* 92 (2004) 947–955.
- [8] J. Riu, A. Maroto, F.X. Rius, Nanosensors in environmental analysis, *Talanta* 69 (2) (2006) 288–301.
- [9] F. Piccinno, F. Gottschalk, S. Seeger, B. Nowack, Industrial production quantities and uses of ten engineered nanomaterials in Europe and the world, *J. Nanoparticle Res.* 14 (2012) 1109, <http://dx.doi.org/10.1007/s11051-012-1109-9>.
- [10] D.B. Warheit, T.R. Webb, K.L. Reed, S. Frerichs, C.M. Sayes, Pulmonary toxicity study in rats with three forms of ultrafine-TiO<sub>2</sub> particles: differential responses related to surface properties, *Toxicology* 230 (2007) 90–104.
- [11] C.M. Sayes, R. Wahi, P.A. Kurian, Y. Liu, J.L. West, K.D. Ausman, D.B. Warheit, V.L. Colvin, Correlating nanoscale titania structure with toxicity: a cytotoxicity and inflammatory response study with human dermal fibroblasts and human lung epithelial cells, *Toxicol. Sci.* 92 (2006) 174–185.
- [12] A. Elsaesser, C.V. Howard, Toxicology of nanoparticles, *Adv. Drug Deliv. Rev.* (2011) <http://dx.doi.org/10.1016/j.jadr.2011.09.001>.
- [13] IARC (International Agency for Research on Cancer), Titanium dioxide group 2B, IARC Monographs on the Evaluation of Carcinogenic Risks to Humans, vol. 9, International Agency for Research on Cancer, World Health Organization, Lyon, France, 2006.
- [14] IARC (International Agency for Research on Cancer), Carbon black, titanium dioxide, and talc, IARC Monographs on the Evaluation of Carcinogenic Risks to Humans, vol. 93, International Agency for Research on Cancer, World Health Organization, Lyon, France, 2010.
- [15] M.A. Gattoo, S. Naseem, M.Y. Arfat, A.M. Dar, K. Qasim, S. Zubair, Physicochemical properties of nanomaterials: implication in associated toxic manifestations, *BioMed. Res. Int.* (2014) <http://dx.doi.org/10.1155/2014/498420>.
- [16] K. Toda, H. Furuse, Extension of Einstein's viscosity equation to that for concentrated dispersions of solutes and particles, *J. Biosci. Bioeng.* 102 (6) (2006) 524–528.
- [17] A. Chandra, V. Patidar, Mansingh, R.K. Kale, Physicochemical and friccohesity study of glycine, l-alanine and l-phenylalanine with aqueous methyltriethylammonium and cetylpyridinium chloride from T = (293.15 to 308.15) K, *J. Chem. Thermodyn.* 65 (2013) 18–28.
- [18] S. Undre, Mansingh, R.K. Kale, Interaction behaviour of trimesoyl chloride derived 1st tier dendrimers determined with structural and physicochemical properties required for drug designing, *J. Mol. Liq.* 182 (2013) 106–120.
- [19] S.M. Ahmadi, G. Dehghan, M.A.H. Feizi, D. JEN, In vitro studies on calf thymus DNA interaction with Quercetin–Palladium (II) complex, International Conference on Bioscience, Biochemistry and Bioinformatics IPCBEE, vol.5, IACSIT Press, Singapore, 2011.
- [20] Q.L. Zhang, J.G. Liu, H. Chao, G.Q. Xue, L.N. Ji, *J. Inorg. Biochem.* 83 (2001) 49–55.
- [21] M. Rahban, A. Divsalar, A.A. Saboury, A. Golestani, Nanotoxicity and spectroscopy studies of silver nanoparticle: calf thymus DNA and K562 as targets, *J. Phys. Chem. C* 114 (2010) 5798–5803.
- [22] C. Silvestri, J.S. Brodbelt, Tandem mass spectrometry for characterization of covalent adducts of DNA with anticancer therapeutics, *Mass Spectrom. Rev.* 2 (2012) 1–20.

- [23] A. Oleksi, A.G. Blanco, R. Boer, J. Usin, J. Aymami, A. Rodger, M.J. Hannon, M. Coll, *Angew. Molecular recognition of a three-way DNA junction by a metallosupramolecular helicate*, *Angew. Chem. Int. Ed. Engl.* 45 (2006) 1227–1231.
- [24] P.R. Reddy, A. Shilpa, *Interaction of DNA with small molecules: role of copper histidyl peptide complexes in DNA binding and hydrolytic cleavage*, *Indian J. Chem.* 49A (2010) 1003–1015.
- [25] M. Sirajuddin, S. Ali, A. Badshah, *Drug DNA interactions and their study by UV-visible, fluorescence spectroscopies and cyclic voltammetry*, *J. Photochem. Photobiol.* 124 (2013) 1–19.
- [26] F. Arjmand, A. Jamsheera, *DNA binding studies of new valine derived chiral complexes of tin (IV) and zirconium (IV)*, *Spectrochim. Acta A* 78 (2001) 45–51.
- [27] C. jin, Y. Tang, X.Y. Fan, X.T. Ye, X.L. Li, K. Tang, Y.F. Zhang, A.G. Li, Y.J. Yang, *In vivo evaluation of the interaction between titanium dioxide nanoparticle and rat liver DNA*, *Toxicol. Ind. Health* 29 (3) (2013) 235–244.
- [28] K. Bhattacharya, M. Davoren, J. Boertz, R.P.F. Schins, Hoffmann, E. Dopp, *Titanium dioxide nanoparticles induce oxidative stress and DNA-adduct formation but not DNA-breakage in human lung cells*, *Part. Fibre Toxicol.* 6 (2009) 17, <http://dx.doi.org/10.1186/1743-8977-6-17>.
- [29] K. Samy El-said, E. Mostafa Ali, K. Kanehira, A. Taniguchi, *Molecular mechanism of DNA damage induced by titanium dioxide nanoparticles in toll-like receptor 3 or 4 expressing human hepatocarcinoma cell lines*, *J. Nanobiotechnol.* 12 (2014) 48, <http://dx.doi.org/10.1186/s12951-014-0048-2>.
- [30] S.J.I. Kang, B.M. Kim, Y.J. Lee, H.W. Chung, *Titanium dioxide nanoparticles trigger p53-mediated damage response in peripheral blood lymphocytes*, *Environ. Mol. Mutagen.* 49 (5) (2008) 399–405, <http://dx.doi.org/10.1002/em.20399>.
- [31] C.I. Xue, J. Wu, F. Lan, W. Liu, X. Yang, F. Zeng, H. Xu, *Nano titanium dioxide induces the generation of ROS and potential damage in HaCaT cells under UVA irradiation*, *J. Nanosci. Nanotechnol.* 10 (12) (2010) 8500–8507.
- [32] G. Pratviel, J. Bernadou, B. Meunier, *DNA and RNA cleavage by metal complexes*, *Adv. Inorg. Chem.* 45 (1998) 251–312.
- [33] N. Shahabadi, S. Kashanian, M. Khosravi, M. Mahdavi, *Multispectroscopic DNA interaction studies of a water-soluble nickel(II) complex containing different dinitrogen aromatic ligands*, *Transit. Met. Chem.* 35 (2010) 699–705.
- [34] R. Indumathy, S. Radhika, M. Kanthimathi, T. Weyhermuller, N.B. Unni, *Cobalt complexes of terpyridine ligand: crystal structure and photocleavage of DNA*, *J. Inorg. Biochem.* 101 (3) (2007) 434–443.
- [35] B. Verma, M. Pardhi, R. Pande, *Experimental and computational study of binding interaction of alkoxy derivatives of N-arylhydroxamic acid with DNA*, *Int. J. Pharm. Pharm. Sci.* 6 (9) (2014) 170–174 (ISSN-0975-149).
- [36] G. Psomas, A. Tarushi, E.K. Efthimiadou, *Synthesis, characterization and DNA-binding of the mononuclear dioxouranium(VI) complex with ciprofloxacin*, *Polyhedron* 27 (2008) 133–138.